PHYSICAL REVIEW C **78**, 041302(R) (2008)

Structure of ^{7}He by proton removal from ^{8}Li with the $(d, {}^3\text{He})$ reaction

A. H. Wuosmaa,[1] J. P. Schiffer,[2] K. E. Rehm,[2] J. P. Greene,[2] D. J. Henderson,[2] R. V. F. Janssens,[2] C. L. Jiang,[2] L. Jisonna,[3] J. C. Lighthall,[1] S. T. Marley,[1] E. F. Moore,[2] R. C. Pardo,[2] N. Patel,[4] M. Paul,[5] D. Peterson,[2] Steven C. Pieper,[2] G. Savard,[2] R. E. Segel,[3] R. H. Siemssen,[6] X. D. Tang,[2] and R. B. Wiringa[2]

[1]*Physics Department, Western Michigan University, Kalamazoo, Michigan 49008-5252, USA*
[2]*Physics Division, Argonne National Laboratory, Argonne, Illinois 60439, USA*
[3]*Physics Department, Northwestern University, Evanston, Illinois 60208, USA*
[4]*Physics Department, Colorado School of Mines, Golden, Colorado 80401, USA*
[5]*Hebrew University, Jerusalem, Israel 91904*
[6]*Kernfysich Versneller Instituut, 9747 AA Groningen, The Netherlands*

(Received 30 June 2008; published 10 October 2008)

We report on a study of the structure of the unbound nucleus ^{7}He utilizing the proton-removal reaction ^{2}H(^{8}Li, ^{3}He)^{7}He. Combining the present results with those of our prior measurements of the neutron-adding reaction ^{2}H(^{6}He, p)^{7}He, a consistent picture emerges for the low-lying excitations in ^{7}He. Specifically, the negative-parity sequence of resonances, in order of excitation energies, is consistent with $3/2^-$, $1/2^-$, and $5/2^-$. The stable-beam reactions ^{2}H(^{7}Li, t)^{6}Li and ^{2}H(^{7}Li, ^{3}He)^{6}He were also measured. The results are compared with the predictions of nuclear structure models, including those of *ab initio* quantum Monte Carlo calculations.

DOI: 10.1103/PhysRevC.78.041302 PACS number(s): 25.60.Je, 21.10.Jx, 21.60.De, 27.20.+n

Evidence for a resonance corresponding to the neutron-unbound ground state of ^{7}He was first observed more than 40 years ago [1]; however, the positions and quantum numbers of excitations in this nucleus have remained uncertain. The excitations of ^{7}He are broad resonances that are difficult to separate. One approach to this problem is to produce this system with complementary reactions that probe different aspects of ^{7}He to clarify the nature of these resonances. Previous single-nucleon transfer reactions leading to ^{7}He have included (d, p) [2,3] and (p, d) [4,5]. Here, we present a study of the one-proton $(d, {}^3\text{He})$ pickup reaction from ^{8}Li.

Excited states in ^{7}He have been the subject of shell-model calculations [6,7] and, more recently, of *ab initio* methods such as quantum Monte Carlo [both variational (VMC) and Green's function (GFMC)] [8,9] and no-core shell model (NCSM) [10–12]. All of these calculations predict the sequence $J^\pi = 1/2^-, 5/2^-, 3/2^-$ for the first three excitations above the $3/2^-$ ground state, with a 2 to 3 MeV gap between the ground and first-excited states. The excitation energies from several calculations are listed in Table I. The resonance properties of excitations of ^{7}He have also been examined using the resonating group method (RGM) [13] and the continuum shell model (CSM) [14]. The position and width of the ground state of ^{7}He are well described by these calculations and both support a broad $1/2^-$ first-excited state near 3 MeV in excitation energy. The predictions of the resonance energies from the CSM and the excitation energies from shell model and GFMC calculations are similar. More recent calculations for the properties of ^{7}He are also available using the Gamow shell model [15], the microscopic cluster model [16], and a complex scaling method [17]. These calculations predict a wider range of excitation energies and, in some cases, different level ordering for ^{7}He resonances.

Recently, the single-particle overlaps leading to spectroscopic factors for nucleon transfer and charge exchange in neutron-rich lithium and helium isotopes have been the focus of a number of experiments [2,18–21]. While, in several cases, data are in reasonable agreement with theory, many uncertainties remain, including the use of unbound wave functions in the distorted-wave Born approximation (DWBA) analysis of the reaction data and the problems of appropriate optical-model parameters describing the interaction with diffuse light nuclei. Table II lists some the calculated spectroscopic factors of the lowest excitations in ^{7}He for neutron-stripping and proton-pickup reactions from VMC calculations, as well as those deduced using older Cohen-Kurath (CK) wave functions [7].

Early experimental evidence for excited states in ^{7}He came from a study of the heavy-ion transfer reaction ^{9}Be(^{15}N, ^{17}F)^{7}He [22], where a resonance at an excitation energy near 3 MeV with a width of $\Gamma = 1.9(2)$ MeV was reported. Two reports of the neutron-pickup reaction ^{1}H(^{8}He, d)^{7}He have appeared [4,5], which also suggest an excitation near $E_X = 3$ MeV decaying to $^4\text{He} + 3n$. This observation suggests that this level decays through the ^{6}He(2^+) state, consistent with an assignment of $J^\pi = 5/2^-$, although the population of that excitation via neutron pickup from the p shell would require either a multistep reaction mechanism or significant f-wave contributions.

Production of ^{7}He in a fragmentation reaction was interpreted as suggesting the presence of a low-lying first-excited state at $E_X \approx 600$ keV [23], which was presumed to have spin and parity $1/2^-$, in disagreement with the higher excitation energy for this configuration suggested by most theories. Data from one of the (p, d) reactions [5] qualitatively support this conjecture. Data from the (d, p) reaction on ^{6}He [2], where a $1/2^-$ state should be strongly excited, were consistent with a broad resonance at $E_X = 2.6$ MeV but no strength was observed at lower excitation energy. Neither was a low-lying resonance seen in recent reports of the charge-exchange reaction ^{7}Li(d, ^{2}He)^{7}He [24,25], or as analog strength in ^{7}Li studied in the (p, n) charge-exchange reaction on ^{6}He to the 0^+ state in ^{6}Li [26].

TABLE I. Excitation energies in MeV for low-lying resonances in ^{7}He from Cohen-Kurath (CK) [7], GFMC, and NCSM calculations and experimental values from Ref. [2] and the present work.

J^π	E_X (CK)	E_X (GFMC)	E_X (NCSM)	E_X (Exp)
$3/2^-$	0.00	0.00	0.0	0.0
$1/2^-$	2.56	2.9(3)	2.3	2.6(0.1) [2]
$5/2^-$	3.64	3.3(2)	3.7	2.9(0.3)
$3/2^-$	3.88	3.8(2)	4.4	–

To gain a better understanding of the properties of ^{7}He, we have studied the $(d, ^3\mathrm{He})$ proton-pickup reaction on ^{8}Li. The spectroscopic factors listed in Table II for the (d, p) and $(d, ^3\mathrm{He})$ reactions leading to ^{7}He show that the reactions are highly selective and lead to different states in ^{7}He, and a comparison of experimental results for these different reactions is informative. For example, neutron stripping via the (d, p) reaction populates only the ground and $1/2^-$ states in ^{7}He, whereas the $(d, ^3\mathrm{He})$ reaction has significant strength for only the ground and $5/2^-$ states. The $1/2^-$ level decays predominantly to the particle-bound ^{6}He ground state, while the $5/2^-$ state decays entirely to the two-neutron unbound first-excited 2^+ state in ^{6}He, thus providing an experimental signature with which to distinguish the two excitations.

The experiment was performed using a ^{8}Li beam produced at the "In-Flight" facility at the ATLAS accelerator at Argonne National Laboratory [27]. This beam was produced by bombarding a cryogenic D_2 gas cell pressurized to 1400 mbar with a 70 pnA beam of ^{7}Li at an energy of 81 MeV. The secondary beam produced from $^2\mathrm{H}(^7\mathrm{Li}, p)^8\mathrm{Li}$ reactions in the gas cell was focused with a 6T superconducting solenoid and then passed through a bunching resonator to optimize its longitudinal emittance. The ^{8}Li ions were then separated from the primary beam using a dipole magnet and mechanical slits. The resulting ^{8}Li secondary beam had an intensity of between 0.7×10^5 and 1.0×10^5 particles per second and an energy of 76 MeV. We observed no contamination of the secondary beam from ^{7}Li primary-beam ions. In a separate measurement, a low-intensity ^{7}Li beam was transported directly to the experiment for test purposes. The beam-spot size was estimated to be approximately 2 mm for the stable-beam measurements and approximately 5 mm for the ^{8}Li-induced reactions.

The ^{7,8}Li ions bombarded a 420 μg/cm^2 deuterated polyethylene $[(CD_2)_n]$ target. The ^{3}He and ^{3}H ejectiles were detected in a set of three annular, double-sided, and segmented silicon strip detectors, subtending laboratory angles ranging from 9° to 48°. The heavier beam-like recoil reaction products, including ^{4,6}He for the ^{8}Li-induced reactions and ^{6}Li and ^{4,6}He from the ^{7}Li-induced reactions, were detected in coincidence with the light ions in an array of four silicon $\Delta E - E$ telescopes covering laboratory polar angles from 1.4° to 7.2° for 92% of the azimuthal range. The $^2\mathrm{H}(^8\mathrm{Li}, t)^7\mathrm{Li}$ reaction was not observed because either the tritons had energies below annular-detector thresholds or the tritons and the ^{7}Li recoils were outside the recoil-coincidence acceptance.

The beam intensity was monitored in two ways. Downstream of the forward $\Delta E - E$ detector array, a 150 μg/cm^2 thick gold foil was used to scatter the unreacted beam into a $\Delta E - E$ monitor telescope at a very forward angle. Also, a sample of ^{7,8}Li ions elastically scattered from the CD_2 target into the $\Delta E - E$ array was recorded. Estimates of the beam intensity from these two methods were consistent. The systematic uncertainty ascribed to the absolute normalization, deriving from uncertainties in the spot size, target thickness, and detector geometry, is estimated to be 10%. Details of other uncertainties in the center-of-mass angle determination from the detector geometry are discussed below. Many aspects of the detector setup were similar to those described in Refs. [2] and [18], permitting a straightforward comparison of the present results with those earlier data. Finally, to assess the backgrounds produced by interactions of the beam with the ^{12}C content of the $(CD_2)_n$ target, data were obtained for ^{7,8}Li incident on a ^{12}C target to provide background data sets with statistics comparable to those obtained with the $(CD_2)_n$ target.

Figure 1 presents excitation-energy spectra for the $^2\mathrm{H}(^7\mathrm{Li}, ^3\mathrm{He})^6\mathrm{He}$ reaction (panels a and b) and the $^2\mathrm{H}(^7\mathrm{Li}, t)^6\mathrm{Li}$ reaction (panels c and d) derived from the energies and angles of light particles detected in the annular detectors. The events in Fig. 1 are obtained with ^{6}He, ^{6}Li, and ^{4}He particles identified in the forward telescope array. The excitation-energy scales are set by shifting the measured Q value by an amount corresponding to the ground-state Q values for the $^2\mathrm{H}(^7\mathrm{Li}, ^3\mathrm{He})^6\mathrm{He}(Q_{\mathrm{gs}} = -4.483$ MeV) and $^2\mathrm{H}(^7\mathrm{Li}, t)^6\mathrm{Li}(Q_{\mathrm{gs}} = -0.993$ MeV) reactions. As the ^{3}He and ^{3}H ions are not distinguished in the annular detectors, for the α-particle coincidence data shown in Figs. 1(b) and 1(d), the identical spectrum appears shifted by the amount appropriate for the ground-state Q value of the $(d, ^3\mathrm{He})$ or (d, t) reaction, respectively.

The solid histograms represent the spectra obtained after subtraction of the contributions from the ^{12}C present in the target. The particle-bound ground state of ^{6}He and the ground and second-excited states in ^{6}Li are clearly seen in Figs. 1(a) and 1(c). In Figs. 1(b) and 1(d) the peaks corresponding to the particle-unbound $^6\mathrm{He}(2^+)$ and $^6\mathrm{Li}(3^+)$ states are present. We attribute the difference in resolution between states populated by the (d, t) and $(d, ^3\mathrm{He})$ reactions in Fig. 1 to the smaller energy straggling for tritons as compared to ^{3}He ions in the $(CD_2)_n$ target.

Excitation-energy spectra from the $^2\mathrm{H}(^8\mathrm{Li}, ^3\mathrm{He})$ $^7\mathrm{He}(Q_{\mathrm{gs}} = -6.960$ MeV) reaction appear in Figs. 2(a)–2(c), which correspond to events where a ^{3}He ion is detected in

TABLE II. Theoretical spectroscopic factors for transitions leading to different final states in ^{7}He from CK and VMC wave functions. The dominant decay mode for each state is also indicated.

J^π	$C^2S[^6\mathrm{He}(d, p)]$		$C^2S[^8\mathrm{Li}(d, ^3\mathrm{He})]$		Decay
	(CK)	(VMC)	(CK)	(VMC)	
$3/2^-$	0.59	0.53	0.80	0.58	$^6\mathrm{He}(0^+) + n$
$1/2^-$	0.69	0.91	0.005	0.009	$^6\mathrm{He}(0^+) + n$
$5/2^-$	0.00	0.00	0.17	0.17	$^6\mathrm{He}(^+) + n$
$3/2^-$	0.06	0.05	0.03	0.003	$^6\mathrm{He}(0^+, 2^+) + n$

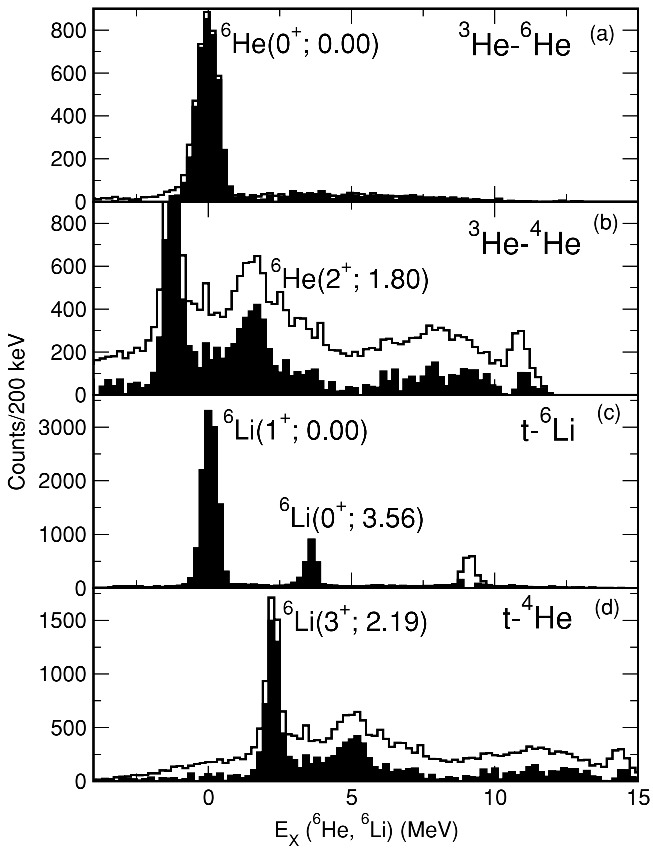

FIG. 1. Excitation-energy spectra from ^{7}Li + ^{2}H interactions derived from t or ^{3}He angles and energies, with those light particles detected in coincidence with (a) ^{6}He, (b) ^{4}He, (c) ^{6}Li, and (d) ^{4}He identified in the forward $\Delta E - E$ array. The excitation-energy scales are adjusted for the ground-state Q value of the ^{2}H(^{7}Li, ^{3}He)^{6}He reaction (a,b) and the ^{2}H(^{7}Li, t)^{6}Li reaction (c,d). The spectra in panels (b) and (d) are identical except for the differing shifts from the different ground-state Q values. The open (solid) histograms represent the spectra before (after) ^{12}C background subtraction.

coincidence with (a) either a ^{4}He or a ^{6}He ion, (b) ^{6}He only, or (c) ^{4}He only. The histograms have the same significance as those in Fig. 1. In Fig. 2(a), the ^{7}He ground state is clearly observed, as is evidence for excited-state strength around $E_X = 3$ MeV. The ^{3}He-^{6}He coincidence spectrum of Fig. 2(b) contains only the ground-state peak. Conversely, in Fig. 2(c) containing ^{3}He-^{4}He events, only the counts at higher excitation energy remain. The distribution is somewhat asymmetric, with counts trending to lower excitation energy that may represent contributions from a multibody continuum. A similar trend may be found in the ^{3}He-^{4}He coincidence data shown in Fig. 1. The Monte Carlo simulations described below suggest a Gaussian profile for the experimental peak shape, and fitting the data in the excitation-energy range of 1 to 5 MeV yields a value of $E_X = 2.9(3)$ MeV and a width of $\Gamma = 2.0(0.3)$ MeV FWHM. The uncertainties are dominated by the limited statistics in the data.

Figure 2 also compares the results from the current measurement with those of the previous study of the ^{2}H(^{6}He, p)^{7}He reaction [2]. Figures 2(d)–2(f) show excitation-energy spectra from Ref. [2] with coincidence requirements the same as those in Figs. 2(a)–2(c). The spectra are qualitatively similar in Figs. 2(a) and 2(d), where coincidences with both He isotopes are included, with a prominent ground-state peak and a broad ($\Gamma \approx 1.0$ MeV) distribution of counts at higher excitation energy. In contrast, in the (d, ^{3}He) reaction, only the ground state remains when ^{6}He coincidences are selected, while for the (d, p) reaction most of the events remain in the broad maximum, as is shown in Figs. 2(b) and 2(e). The yield from the (d, p) reaction leading to neutron-unbound resonances in ^{6}He is very small as seen in Fig. 2(f). Monte Carlo simulations for the two reactions based on realistic detector geometries reveal similar α-particle coincidence efficiencies. The two reactions evidently probe different components of the wave function of the ^{7}He residual nucleus. The remaining yield to high excitation in the (d, p) reaction is in coincidence with ^{4}He, which would be expected if the decay is to the 2^{+} state of ^{6}He, and at higher excitation energy than the bump in (d, ^{3}He).

These observations are consistent with expectations for the two reactions as summarized by the spectroscopic factors given in Table II. In the (d, p) reaction, only the ground and first-excited states have large spectroscopic strength and both decay either entirely or predominantly to the particle-bound ground state of ^{6}He. The absence of any yield at high excitation energy in Fig. 2(b) is consistent with a $5/2^{-}$ resonance decaying entirely to the ^{6}He(2^{+}) state. Thus, these two data sets suggest $3/2^{-}$ ground and $1/2^{-}$ first-excited states populated in neutron stripping and the ground and $5/2^{-}$ second-excited states in proton pickup.

We have extracted angular distributions for the states populated in the ^{2}H(^{8}Li, ^{3}He)^{7}He reaction, as well as for the levels populated in the ^{2}H(^{7}Li, ^{3}He)^{6}He and ^{2}H(^{7}Li, t)^{6}Li calibration reactions. Because of the finite beam-spot and detector-segment size, the transformation to center-of-mass angle as well as the detector response must be deconvoluted from the laboratory detector position using a Monte Carlo unfolding procedure. The simulations take into account the beam-spot size, realistic detector geometries and resolutions, missing detector segments, and recoil-coincidence efficiency. The response function is extremely sensitive to detector geometry when the maximum laboratory angle for the light ejectile is near the overlap region between two annular detectors. This sensitivity makes the deconvolution process less reliable for some states populated in the calibration reactions, as discussed below.

Figures 3(a)–3(c) present angular distributions for the reactions leading to the ^{6}He(0^{+}) ground state, the ^{6}Li(1^{+}) ground state, and the ^{6}Li(0^{+}) excited state, respectively. For the reaction ^{2}H(^{7}Li, ^{3}He)^{6}He(0^{+}), data exist at nearly the same bombarding energy from Ref. [28] and these are plotted in Fig. 3(a) as square symbols. The cross section at the peak of the angular distribution is in good agreement with previous results, giving us confidence in the normalization procedure. The deviations between the two data sets at larger center-of-mass angles likely arise from the sensitivities in the response function described above. No comparable data for the (d, t) reaction on ^{7}Li are available at this bombarding energy; however, the measured cross sections for the reactions from ^{7}Li

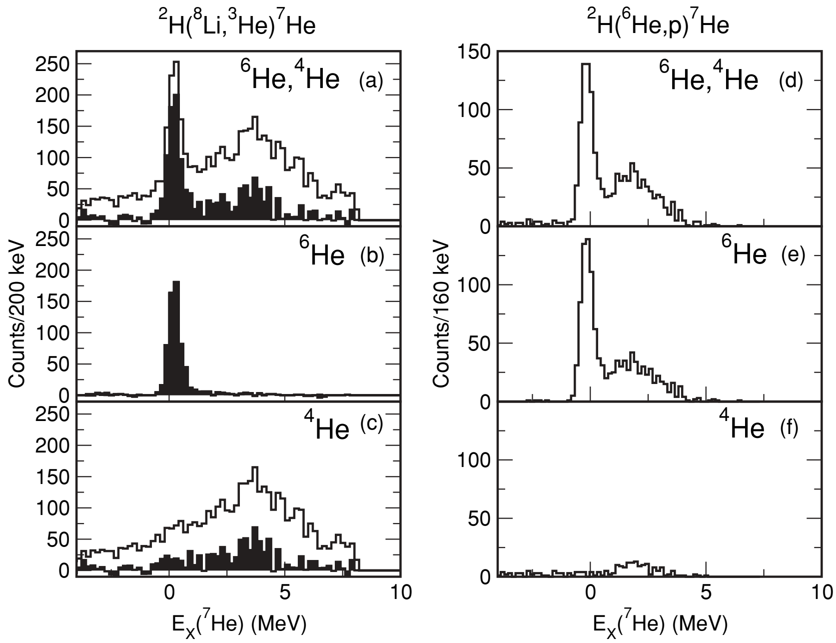

FIG. 2. Excitation-energy spectra for the ^{2}H(^{8}Li, ^{3}He)^{7}He reaction are shown in panels (a)–(c) corresponding to coincidences between a particle in the segmented detector array and (a) identified ^{4,6}He ions, (b) ^{6}He ions only, and (c) ^{4}He ions only. Excitation-energy spectra for the ^{2}H(^{6}He, p)^{7}He reaction are shown in panels (d)–(f) corresponding to coincidences between a particle in the segmented detector array and (d) identified ^{4,6}He ions, (e) ^{6}He ions only, and (f) ^{4}He ions only. The open (solid) histograms in panels (a)–(c) represent the spectra before (after) ^{12}C background subtraction.

to the two analog 0^+ states in ^{6}Li and ^{6}He differ by a factor of approximately two as expected from isospin arguments [29]. Figures 3(d) and 3(e) display angular distributions for the ground-state and $5/2^-$ excitations in ^{7}He. The ^{3}He particles from the ^{2}H(^{8}Li, ^{3}He)^{7}He reaction are limited to more forward laboratory angles and the center-of-mass angle transformations are not sensitive to the detector geometry. For the $5/2^-$ state, the yield is determined from the integral of the spectrum at each angle between $E_X = 1.5$ and 5.0 MeV.

The curves in Fig. 3 illustrate the results of optical-model calculations using the finite-range DWBA code PTOLEMY [30], with optical-model parameters for the entrance and exit channels taken from Refs. [31] (Set 2) and [32], respectively. The bound-state wave functions at both vertices were computed from the overlaps of VMC wave functions. In each case, the calculation is normalized to the data at the angular-distribution peak. The shapes of the calculated angular distributions are in reasonable agreement with the data and consistent with $l = 1$ transitions, as expected in these nuclei.

Table III lists "experimental" and theoretical spectroscopic factors for the transitions of Fig. 3. The theoretical C^2S values represent the spectroscopic overlaps calculated using the VMC method. The experimental numbers are obtained by comparing

TABLE III. Comparison of experimental and theoretical spectroscopic factors for the (d, t) and $(d, {}^3\text{He})$ reactions; σ denotes the cross section at the angular-distribution maximum.

Reaction	σ (Exp) (mb/sr)	C^2S (Exp)[a]	C^2S (VMC)
^{7}Li(d, ^{3}He)^{6}He(0^+)	12.3(2.0)	0.44(6)	0.42
^{7}Li(d, t)^{6}Li(1^+)	41.2(6.0)	0.74(11)	0.68
^{7}Li(d, t)^{6}Li(0^+)	5.6(0.9)	0.19(3)	0.21
^{8}Li(d, ^{3}He)^{7}He($3/2^-$)	4.5(0.9)	0.36(7)	0.58
^{8}Li(d, ^{3}He)^{7}He($5/2^-$)	1.0(0.5)	0.29(15)	0.17

[a]Values obtained from $(\sigma_{\text{Exp}}/\sigma_{\text{DWBA}}) \times 0.32$.

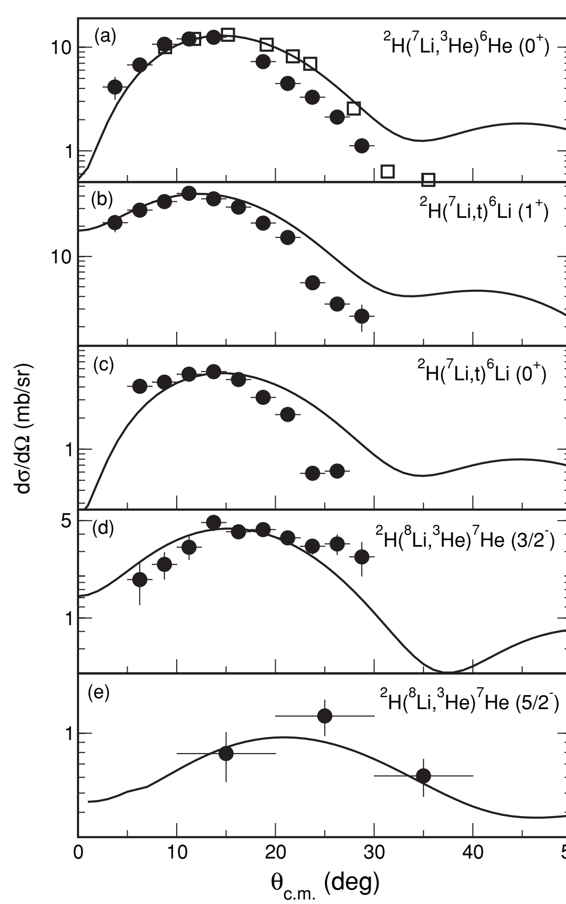

FIG. 3. Angular distributions for (a) the ^{2}H(^{7}Li, ^{3}He)^{6}He(0^+) transition, (b,c) the ^{2}H(^{7}Li, t)^{6}Li ground-state and second-excited-state transitions, respectively, and (d,e) the ^{2}H(^{7}Li, ^{3}He)^{6}He reaction to the $3/2^-$ ground state and $5/2^-$ resonance, respectively. The horizontal error bars in all cases reflect the center-of-mass angle binning of the data. The curves represent DWBA calculations described in the text.

the calculated DWBA cross section with the measured value at the peak of the angular distribution. The DWBA predictions are sensitive to variations in the optical-model parameters and cannot be trusted to provide an absolute determination of the cross section. The relative cross sections for different transitions, calculated using the same potential parameters, should be more reliable. To compare the experimental values with the predictions of the VMC, the measured spectroscopic factors in Table III contain an overall normalization factor of 0.32 obtained from an error-weighted average of the individual ratios between the experimental and the VMC numbers. In addition to the uncertainties inherent in representing the distortion of reaction channels to loosely bound or unstable final nuclei by "normal" optical-model parameters, there are the experimental uncertainties that include statistical errors, the uncertainty in the absolute determination of the beam intensity, and the estimated systematic uncertainty arising from the Monte Carlo deconvolution of the angular-distribution data. Except for the overall normalization factor, the measured and calculated spectroscopic factors are in good agreement, indicating that the trends in the data are well reproduced by the calculations. In particular, although the experimental uncertainty is large, the result for the suggested $5/2^-$ state is in agreement with the prediction and supports this identification. Michel *et al*. have studied the influence of the Wigner cusp phenomenon on the spectroscopic factors for nucleon transfer in weakly bound nuclei, suggesting that these factors may be reduced significantly for states near threshold as compared to expectations from a conventional shell-model approach [33]. The statistics for the $5/2^-$ state are, however, insufficient to quantitatively explore such effects.

In summary, we have made considerable progress in understanding the excitations of the unbound nucleus ^{7}He by combining our results from the ^{2}H(^{8}Li, ^{3}He)$\,^{7}$He reaction with our earlier data from the ^{2}H(^{6}He, p)$\,^{7}$He reaction. The results are consistent with the sequence of negative-parity states $3/2^-$, $1/2^-$, $5/2^-$ at $E_X = 0.0$, 2.6, and 3.0 MeV suggested by most nuclear models. The energies of these levels are also consistent with the results of these calculations. The trends in the relative spectroscopic factors are also in good agreement with the values obtained from the VMC calculations.

This work was supported by the U. S. Department of Energy, Office of Nuclear Physics, under Contracts DE-FG02-04ER41320 (WMU), DE-AC02-06CH11357 (ANL), and DE-FG02-98ER4106 (NU).

[1] R. H. Stokes and P. G. Young, Phys. Rev. Lett. **18**, 611 (1967).
[2] A. H. Wuosmaa *et al*., Phys. Rev. C **72**, 061301(R) (2005).
[3] M. S. Golovkov *et al*., Phys. At. Nucl. **64**, 1244 (2001).
[4] A. A. Korsheninnikov *et al*., Phys. Rev. Lett. **82**, 3581 (1999).
[5] F. Skaza *et al*., Phys. Rev. C **73**, 044301 (2006).
[6] A. A. Wolters, A. G. M. van Hees, and P. W. M. Glaudemans, Phys. Rev. C **42**, 2062 (1990).
[7] S. Cohen and D. Kurath, Nucl. Phys. **73**, 1 (1965); Nucl. Phys. **A101**, 1 (1967); D. Kurath (private communication).
[8] S. C. Pieper and R. B. Wiringa, Annu. Rev. Nucl. Part. Sci. **51**, 53 (2001).
[9] S. C. Pieper, R. B. Wiringa, and J. Carlson, Phys. Rev. C **70**, 054325 (2004).
[10] P. Navrátil and B. R. Barrett, Phys. Rev. C **54**, 2986 (1996).
[11] P. Navrátil and B. R. Barrett, Phys. Rev. C **57**, 3119 (1998).
[12] P. Navrátil, Phys. Rev. C **70**, 054324 (2004).
[13] J. Wurzer and H. M. Hofmann, Phys. Rev. C **55**, 688 (1997).
[14] A. Volya and V. Zelevinsky, Phys. Rev. Lett. **94**, 052501 (2005).
[15] G. Hagen, M. Hjorth-Jensen, and Jan S. Vaagen, Phys. Rev. C **71**, 044314 (2005).
[16] A. Adahchour and P. Descouvemont, Phys. Lett. **B639**, 447 (2006).
[17] T. Myo, K. Katō, and K. Ikeda, Phys. Rev. C **76**, 054309 (2007).
[18] A. H. Wuosmaa *et al*., Phys. Rev. Lett. **94**, 082502 (2005).
[19] H. B. Jeppesen *et al*., Phys. Lett. **B635**, 17 (2006).
[20] R. Kanungo *et al*., Phys. Lett. **B660**, 26 (2007).
[21] F. Beck *et al*., Phys. Lett. **B645**, 128 (2007).
[22] H. G. Bohlen *et al*., Phys. Rev. C **64**, 024312 (2001).
[23] M. Meister *et al*., Phys. Rev. Lett. **88**, 102501 (2002).
[24] D. Frekers, Nucl. Phys. **A731**, 76 (2004).
[25] N. Ryezayeva *et al*., Phys. Lett. **B639**, 623 (2006).
[26] G. Rogachev *et al*., Phys. Rev. Lett. **92**, 232502 (2004).
[27] B. Harss *et al*., Rev. Sci. Instrum. **71**, 380 (2000).
[28] R. H. Stokes and P. G. Young, Phys. Rev. C **3**, 984 (1971).
[29] P. T. Debevec, G. T. Garvey, and B. E. Hingerty, Phys. Lett. **B34**, 497 (1971).
[30] M. H. Macfarlane and S. C. Pieper (Argonne National Laboratory Report ANL-76-11, Rev. 1, 1978).
[31] J. P. Schiffer *et al*., Phys. Rev. **164**, 1274 (1967).
[32] R. L. Dixon and R. D. Edge, Nucl. Phys. **A156**, 33 (1970).
[33] N. Michel, W. Nazarewicz, and M. Ploszajczak, Phys. Rev. C **75**, 031301(R) (2007).